

Branching ratios of ${}^9\text{C}$ to low lying states in ${}^9\text{B}$

D. Mikolas, B. A. Brown, W. Benenson, L. H. Harwood, E. Kashy, J. A. Nolen, Jr., B. Sherrill, J. Stevenson, J. S. Winfield, and Z. Q. Xie

Department of Physics and Astronomy and National Superconducting Cyclotron Laboratory, Michigan State University, East Lansing, Michigan 48824

R. Sherr

Department of Physics, Princeton University, Princeton, New Jersey 08540

(Received 7 May 1987)

We report the first observation of the beta decay of ${}^9\text{C}$ to the ground state and to two low-lying excited states of ${}^9\text{B}$. Branching ratios to these states were measured, and a previously reported branch to a level near 12 MeV was confirmed. The branching ratio to the $J^\pi = \frac{3}{2}^-$ ground state is $60 \pm 10\%$, and the branching ratios to the narrow $\frac{5}{2}^-$ level at 2.36 MeV and to the broad $\frac{1}{2}^-$ level near 2.9 MeV are $17 \pm 6\%$ and $11 \pm 5\%$, respectively. Because of the three-body nature of the ${}^9\text{B}$ decay, the ${}^9\text{C}$ ions were implanted in the active volume of silicon detectors, and the total decay energies of the states in ${}^9\text{B}$ were directly measured. We compare these results to shell model calculations, to the analog decay of ${}^9\text{Li}$ to ${}^9\text{Be}$, and to the ${}^9\text{Be}(p,n){}^9\text{B}$ reaction. The comparison to ${}^9\text{Li}$ decay indicates an asymmetry in the beta-decay matrix elements to the $\frac{5}{2}^-$ level larger than any such asymmetry previously observed.

I. INTRODUCTION

The beta-delayed proton precursors with $T_z = -\frac{3}{2}$, $A = 4n + 1$ ($n = 2, 3, \dots$) have been extensively studied, and delayed proton activity from every member of this group from ${}^9\text{C}$ to ${}^{61}\text{Ge}$ has been measured.^{1,2} Most delayed proton spectra from these nuclei show a complicated structure with many peaks, reflecting transitions to discrete narrow levels. In the case of ${}^9\text{C}$, (see Fig. 1) the delayed proton spectrum is dominated by a continuum of proton energies.^{3,4} In addition, the data below about 3 MeV of Refs. 3 and 4 were contaminated by electron pileup.⁵ This prevented the measurement of most of the experimental beta decay strength to ${}^9\text{B}$, which is expected to lie below this experimental cutoff. Furthermore, the ${}^9\text{C}$ beta-delayed proton spectrum is difficult to interpret itself, because unknown fractions of the decay energy are carried away by the two alpha particles. The decay of the ground state of ${}^9\text{B}$ generates a proton with a kinetic energy of only 0.16 MeV,⁶ and the first negative-parity excited state ($\frac{5}{2}^-$ at 2.360 MeV), while it is relatively narrow, decays less than 1% of the time by proton emission to the ground state of ${}^8\text{Be}$.⁷ It instead decays mainly through broad intermediate states leading to a continuum of proton energies.

The problem of the spread in proton energies becomes worse for the higher excitation energies. More decay channels (which can involve excited states in the intermediate fragment) become energetically allowed, and enough phase space becomes available for many of these channels to be populated with significant probability. In this case the proton energy spectrum does not directly reflect the excitation spectrum in ${}^9\text{B}$, since all paths involve decays to three particles ($2\alpha + p$). Even for a fixed excitation in ${}^9\text{B}$, different particle decay channels which

involve states in ${}^8\text{Be}$ and ${}^5\text{Li}$ will generate different proton spectra that can be quite broad. The breakup of the ${}^9\text{B}$ nucleus promptly into three particles is also possible. Therefore, to measure the branching of ${}^9\text{C}$ decay requires a method that detects the population and excitation energies of the ${}^9\text{B}$ levels directly, independent of the decay modes of these states.

In the present experiment, we used the technique of implantation of the delayed particle precursor, ${}^9\text{C}$, within a silicon detector. This method was first used by Chen *et al.*⁸ to investigate the decay of ${}^9\text{Li}$, the mirror nucleus of ${}^9\text{C}$. In that experiment, the excited states of ${}^9\text{Be}$ decayed to $2\alpha + n$, but only the sum of the two α particle energies was measured. The delayed neutron energy spectrum was recorded in a separate experiment.⁸ The excitation energy spectrum in the ${}^9\text{Be}$ nucleus could be inferred from the data only with the use of specific assumptions about the particle decay for each state. The implantation technique was also used by Barnes and Nichols⁹ to make a precise measurement of the β -delayed breakup of the second excited state of ${}^{12}\text{C}$ into three α particles. In this case, as in the case of ${}^9\text{B}$ decay, all the decay particles are charged, and as long as they are completely contained in the silicon, the total decay energy of the nucleus is measured, independently of the decay mode.

The energy deposited in the detector in which both the ${}^9\text{C}$ nucleus decays and the ${}^9\text{B}$ decay fragments stop is the sum of the excitation energy of the ${}^9\text{B}$ nucleus, of the ground state breakup energy of ${}^9\text{B}$ (0.28 MeV), and of a small contribution from the energy loss of the beta particle. Because of the low energies of the alpha particles and the proton, the fraction of the energy loss to nonionizing processes in the silicon must be considered, since these processes will not contribute to the measured ener-

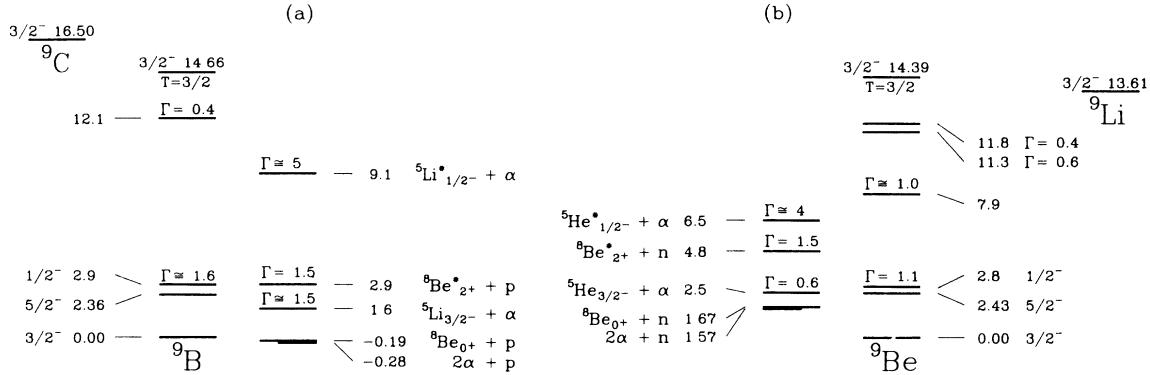


FIG. 1. Relative mass and excitation energies of known and presumed $1/2^-$, $3/2^-$, and $5/2^-$ levels, relevant to beta decay in mass 9, and particle decay thresholds of those levels. All energies in (a) are relative to the ground state mass of ${}^9\text{B}$ (atomic mass excess 12.4158 ± 0.001 MeV) and those in (b) are relative to the ground state of ${}^9\text{Be}$ (11.3477 ± 0.0004). All ground state masses are taken from Wapstra *et al.* (Ref. 58). Energies and widths of excited states are all from Ajzenberg-Selove (Ref. 6), except those of the 2.9 and 12.1 MeV levels in ${}^9\text{B}$, which are discussed in the present work.

gy in the silicon. We estimate that this pulse height defect should lie between 2 and 8 keV per particle^{10,11} (depending on the lab energy of each), and results in only a slight broadening of the peaks that will not significantly affect the following analysis. Since the direction of the particles with respect to the silicon crystal axes cannot be controlled, large pulse height anomalies are possible for particles which channel in the silicon lattice. We assume that the probability of emission of a particle in a direction sufficiently close to any channeling axis is small.

We have expanded upon this technique by using a multidetector telescope. This provides a way to subtract the contribution of the beta particle from the spectrum and thus allows the use of thicker detectors to contain the charged particle energy. It also provides a simple way to check on the containment of charged particles and a potential method to distinguish different decay modes.

The delayed proton data of Hardy *et al.*³ and Esterl *et al.*⁴ contain peaks at roughly 9 and 12 MeV center-of-mass energy, based on the proton decay to the ground state of ${}^8\text{Be}$. These could originate from the decay of two different states in ${}^9\text{B}$, or a single state at 12 MeV which proton decays to both the ground state and first excited state of ${}^8\text{Be}$ (as suggested by the authors). Since our technique measures the excitation in the ${}^9\text{B}$ nucleus directly, there can be no ambiguity of this type. The implantation technique also allows the number of nuclei imbedded in the silicon to be counted, which permits absolute branching ratio measurements.

In the following section, we will describe the experimental procedure of obtaining the beta-delayed charged-particle spectra for ${}^9\text{C}$ decay. In Sec. III we outline the details of the analysis of the data, and methods and assumptions used in obtaining the branching ratios. In Secs. IV and V we discuss previously published data on the beta decay of ${}^9\text{Li}$ and the ${}^9\text{Be}(p,n){}^9\text{B}$ reaction, respectively. In Sec. VI, shell model calculations of beta-decay rates of ${}^9\text{C}$ and ${}^9\text{Li}$, the ${}^9\text{Be}(p,n){}^9\text{B}$ relative cross sections, and the beta-delayed particle de-

decay modes in the mass 9 system are presented. We discuss the connections between all of these data and calculations in Sec. VII, and conclude with suggestions for further experiments in Sec. VIII.

II. EXPERIMENT

A 91 mg/cm² Ni target was bombarded by an $E/A=35$ MeV ${}^{12}\text{C}^{4+}$ beam from the $K=500$ cyclotron at the National Superconducting Cyclotron Laboratory. The Reaction Product Mass Separator (RPMS) (Refs. 12 and 13) was used to separate ${}^9\text{C}$ fragments from the other reaction products emerging at a scattering angle of 3° .

A thin kapton window separated the vacuum of the RPMS from the focal plane, which is in air. The focal plane of the RPMS was equipped with slits to select particles of a given mass/charge ratio (m/q), a position-sensitive proportional counter, and a four element silicon detector telescope. The telescope is schematically illustrated in Fig. 2. It consisted of two 400 μm thick surface barrier detectors and two lithium drifted silicon detectors with thicknesses of 1 and 5 mm. These will be referred to as ΔE , $E1$, $E2$, and $E3$, respectively. The energy response of the electronics was measured to 5% accuracy by means of a calibrated pulser.

Approximately 6000 ${}^9\text{C}$ ions stopped in $E1$, and 4000 in $E2$ in 12 h of data taking with an average beam current of 60 nA. Ions were identified by their energy loss in each detector. The identification was verified by an m/q determination from focal plane position. Other ions which stopped in the detectors were mostly ${}^8\text{B}$ nuclei or scattered beam particles (~ 2000 and ~ 5000 events, respectively). The implantation depth profile of the ${}^9\text{C}$ ions in the silicon was adjusted by means of aluminum absorbers in front of the defining slits so that any variation in the containment of high energy protons could be explored. The range distribution of ${}^9\text{C}$ ions calculated from the total energy measurement is also illustrated in Fig. 2.

The cyclotron beam was turned off within 40 μs of the arrival of an ion (by means of a fast phase shifter in the

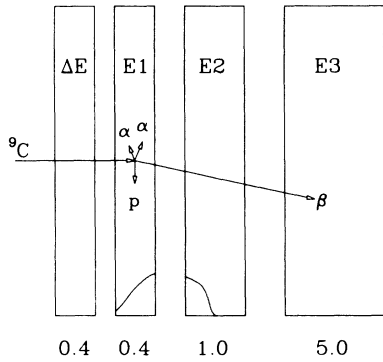


FIG. 2. A schematic diagram of the silicon detector telescope used at the RPMS focal plane. A ${}^9\text{C}$ ion is identified in the telescope, and comes to rest in $E1$ or $E2$. When ${}^9\text{C}$ decays, the β particles, with energies distributed between 0 and 15.5 MeV, usually leave the silicon detector in which the decay occurs, and sometimes enter other elements. The daughter nucleus, ${}^8\text{B}$, always breaks up into two α particles and a proton. The implanted ${}^9\text{C}$ range distribution is indicated in the bottom of $E1$ and $E2$. The thicknesses of the detectors in mm are indicated under each element.

rf transmitter of one of the three “dees” of the cyclotron), and the gain of the silicon detector preamplifiers increased by a factor of 10 for a 480 ms period, approximately four half-lives of ${}^9\text{C}$. The detection of an ion in the focal plane telescope will be referred to as a “beam-on” event, and all events during the following 480 ms period as “beam-off” events. After the beam was turned off and the preamplifiers allowed to stabilize (16 ms), a beam-off event was triggered by signals above a discriminator level, set near 200 keV, from any one of the last three silicon detectors. A scaler module that counted

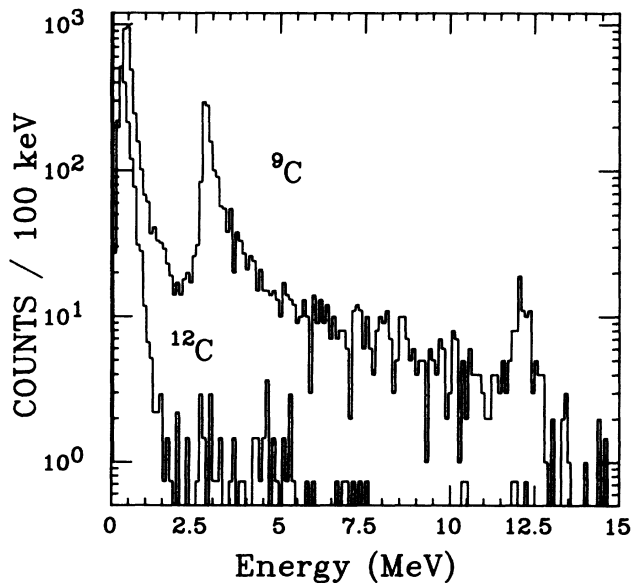


FIG. 3. The beam-off energy spectra associated with ${}^9\text{C}$ and ${}^{12}\text{C}$ ions recorded in $E1$. The spectrum associated with ${}^{12}\text{C}$ has been normalized to the same number of beam-on events as the ${}^9\text{C}$ spectrum.

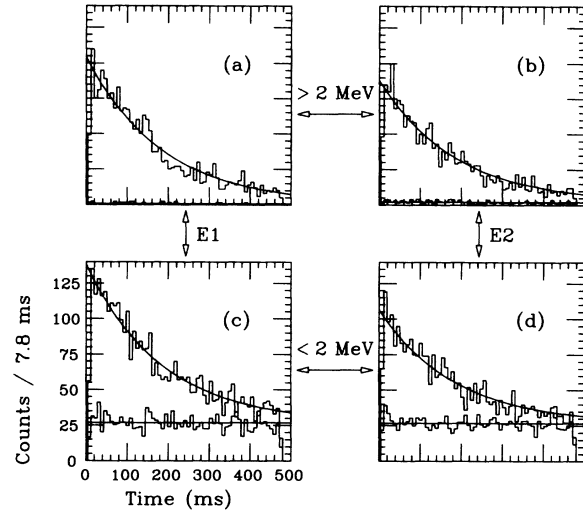


FIG. 4. Time spectra of beam-off events after the arrival of ${}^9\text{C}$ ions in $E1$ and in $E2$, in which the signal in that detector was above or below 2.0 MeV. For each of the four combinations, a histogram of events following the arrival of a ${}^{12}\text{C}$ is also included, to illustrate the background rate. The smooth curves are not direct fits to these data. They are described in Sec. III.

pulses from a 262 kHz quartz oscillator was cleared by a beam-on event, and was read but not cleared for the subsequent beam-off events. Thus the time between the beam-on event and each of the following beam-off events could be determined. The data were recorded event by event on magnetic tape. Each beam-on event could be directly matched with the set of subsequent beam-off events during off-line analysis.

III. ANALYSIS

The energy spectrum of beam-off events for which a ${}^9\text{C}$ ion stopped in $E1$ is shown in Fig. 3. The beam-off spectrum associated with ${}^{12}\text{C}$ ions, normalized to the same number of beam-on events, is also included in the figure. The ${}^{12}\text{C}$ spectrum was used to define the background spectrum. Sources of background include residual beta activity within and near the silicon detectors and electrical noise.

Time spectra of events in each detector associated with ${}^9\text{C}$ or ${}^{12}\text{C}$ are shown in Figs. 4(a)–4(d). The events are further divided into groups of those for which the beam-off signal in the detector of interest was above and those for which it was below 2 MeV. The area of the corresponding regions in the decay spectra in $E1$ and $E2$, associated with ${}^9\text{C}$ and ${}^{12}\text{C}$, above and below 2 MeV were used to generate constant-background and exponential-plus-constant-background curves, and these results are superimposed on the data in Fig. 4. The area of the appropriate region from the normalized ${}^{12}\text{C}$ associated energy spectrum, shown in Fig. 3, is used for the constant background measurement, while the difference between the areas from the ${}^9\text{C}$ and the normalized ${}^{12}\text{C}$ spectrum is used to determine the coefficient of the exponential decay. The previously-measured half-life^{4,6,14}

of 126.5 ± 1.0 ms is used throughout this analysis. As can be seen in Fig. 4, the agreement is good. This indicates that the background is indeed independent of time, and that the separate contributions to the energy spectra from ${}^9\text{C}$ and background have been determined correctly.

The efficiency of the system for the detection of the decay of ${}^9\text{C}$ nuclei was 87% in $E1$ and 94% in $E2$, after correction for finite counting time and dead time. The missing decays are ascribed to the decay of ${}^9\text{B}$ in its ground state, where the total energy released was small, and near the thresholds of the constant fraction discriminators used in the experiment.

The $E2$ detector is much thicker than $E1$, and most of the ${}^9\text{C}$ ions that entered it came to rest close to its front surface. The beta particles leaving $E2$ through the front traversed only a few hundred microns of silicon, while those leaving the back, a minimum of $800 \mu\text{m}$. This makes the peaks in $E2$ (not shown) broader than their counterparts in $E1$ (Fig. 3) by shifting half of the events higher in energy by about 300 keV on average. If our description of the threshold problem is correct, about half of the counts in $E2$ associated with the decay to the ground state should then lie well above the threshold level of the constant fraction discriminator, in a region where the efficiency problem should not occur. This would make the number of undetected decays in $E2$ roughly half of that in $E1$, which conforms with the measured efficiencies, and supports the conclusion that the missing counts are associated with the ground state branch.

Shell model calculations (discussed in Sec. VI) indicate that the decay of ${}^9\text{C}$ should most often populate the three lowest negative parity states in ${}^9\text{B}$ (including the ground state) with roughly equal Gamow-Teller strength. (See Table I.) However, of these three levels,

only the ground state and one excited state branch are evident in Fig. 3. While the ground state¹⁵ and first $\frac{5}{2}^-$ level⁷ in ${}^9\text{B}$ are narrow, it is reasonable to believe that the first $\frac{1}{2}^-$ level in ${}^9\text{B}$ is broad. As discussed in Sec. V, there is evidence for this broad state near 2.7 MeV in the ${}^9\text{Be}(p,n){}^9\text{B}$ spectrum. In the mirror nucleus ${}^9\text{Be}$, the level near 2.9 MeV has a width of roughly 1.0 MeV. (See Table II for both nuclei.) The decay of ${}^9\text{C}$ to a level in ${}^9\text{B}$ with a width of 1.5 MeV would be obscured in our spectrum by the beta energy loss associated with the nearby $\frac{5}{2}^-$ state. Two techniques described below were developed to reduce this effect in order to search for this broad level.

A simulation of the beta energy-loss spectrum was generated by a Monte Carlo routine based on the relation⁹

$$P(E)\delta E = \begin{cases} \frac{E_0}{E^2} \delta E, & E \geq E_0 \\ 0, & E < E_0, \end{cases} \quad (1)$$

where $E_0 = D(dE/dX)_B$, and D is the distance from each implanted ion to the face of the silicon detector from which the beta particle will emerge, as calculated from the beam-on energy of the implanted ion. An effective $(dE/dX)_B$ of 0.5 MeV/mm in Si was found to fit the energy loss in $E1$ and $E2$ from decays in $E1$. This value is about 30% larger than that for a minimum ionizing particle in Si, but, as determined by Barnes and Nichols,⁹ a larger value is expected due to multiple Coulomb scattering in the finite thickness of the detector. The distribution was further broadened to take into account the variability in the pulse height defect associated with the distribution of energies of the three particles, an intrinsic 100 keV resolution of the silicon detec-

TABLE I. Measured and predicted Gamow-Teller beta decay strengths to the lowest $\frac{3}{2}^-$, $\frac{5}{2}^-$, and $\frac{1}{2}^-$ states in mass 9. (BR) denotes branching ratio.

Reference	$\frac{3}{2}^-$ (ground state)		$\frac{5}{2}^-$		$\frac{1}{2}^-$	
	BR (%)	$B(\text{GT})^a$	BR (%)	$B(\text{GT})^a$	BR (%)	$B(\text{GT})^a$
${}^9\text{C}$ experimental						
This work	60 ± 10	0.033 ± 0.006	17 ± 6	0.020 ± 0.007	11 ± 5	0.016 ± 0.007
$A=9$ shell model calculations						
(6-16) 2BME (Ref. 35)		0.035		0.030		0.016
Millener (Ref. 36)		0.046		0.028		0.020
Kumar (Ref. 37)		0.014		0.066		0.010
(8-16) POT (Ref. 35)		0.086		0.039		0.080
${}^9\text{Li}$ experimental						
Nefkens <i>et al.</i> (Ref. 57)	60 ± 10	0.036 ± 0.006				
Macefield <i>et al.</i> ^{b,c} (Ref. 21)			33 ± 5	0.051 ± 0.008	17 ± 5	0.032 ± 0.009
Chen <i>et al.</i> ^b (Ref. 8)	65.0 ± 2.7	0.039 ± 0.002	32.0 ± 3.7	0.049 ± 0.006	3.0 ± 2.3	0.006 ± 0.001
Björnstad <i>et al.</i> (Ref. 26)	50 ± 4	0.030 ± 0.002				
Langevin <i>et al.</i> ^b (Ref. 27)	50.5 ± 5	0.030 ± 0.002	34 ± 4	0.052 ± 0.006	10 ± 2	0.019 ± 0.004

^a $B(\text{GT})$ values are calculated from Eqs. (3) and (4) of Sec. III.

^bSee Table II for the assumed particle decay branches of these states used by each author to extract a measured branching ratio.

^cThe listed branching ratios have been adjusted from the published values for a ground state branch of 50% as described in the text. The $B(\text{GT})$ values are calculated (see footnote a) based on the adjusted branching ratio.

tor and associated electronics, and the width of the particular state.

The solid line in Fig. 5 shows the simulation of the peak shapes for the branches to the ground state and $\frac{5}{2}^-$ level, with about 2450 and 900 decays, respectively, in $E1$. The difference between the ${}^9\text{C}$ decay data (after background subtraction) and the simulation is shown in the inset. While the subtraction leaves almost 0 counts in the vicinity of the ground state decay, a broad residual yield near 3 MeV is clearly evident. This gives a ratio of strengths between the decay to the $\frac{5}{2}^-$ state, and of the decay to the energy range of 2.0 and 4.4 MeV in the subtracted spectrum (not including the $\frac{5}{2}^-$ state) of 1.9. This broad distribution probably represents the population of the $\frac{1}{2}^-$ level in ${}^9\text{B}$ discussed above.

To confirm the presence of the broad level, and to better separate the strength from that of the $\frac{5}{2}^-$ level, a corrected energy spectrum of ${}^9\text{C}$ decay in $E1$ was generated. This was accomplished by modifying the off-line analysis code to require the beta particle to pass from $E1$ through $E2$ and into $E3$. In this case the effective energy loss of each beta in a detector with a thickness of 1 mm was measured for each event by the signal in $E2$. The contribution of the beta to be subtracted from the $E1$ signal for each event is scaled from the energy loss in $E2$ for that event by

$$\Delta E1_\beta = \frac{(400\mu - \text{Range})}{1 \text{ mm}} E2, \quad (2)$$

The corrected $E1$ spectrum is histogrammed, and is shown in Fig. 6 after background subtraction (the background was generated by applying the same process to the ${}^{12}\text{C}$ data). Here the broad state clearly shows up. The lack of a similar structure above the ground state rules out any anomalous beta energy loss tail as the source of the broad distribution. These data suggest that the $\frac{5}{2}^-$ level is populated 1.1 times as frequently as the $\frac{1}{2}^-$ level. In order to determine this ratio, we have assumed that the two peak channels near 2.5 MeV in Fig. 6 contain all of the $\frac{5}{2}^-$ strength, and that the contribution to these two channels from the decay of the $\frac{1}{2}^-$ level is equal to the sum of the two channels immediately above and below the two peak channels. Combining this with the previous value, we estimate that the true ratio of $\frac{5}{2}^-$ to $\frac{1}{2}^-$ branching is 1.5 ± 0.5 . The error bars are not statistical in origin, but were chosen to be consistent with both measurements, reflecting the uncertainty in the methods used to separate the strength to the $\frac{1}{2}^-$ from that of the $\frac{5}{2}^-$.

In order to obtain the actual branching ratio for the $\frac{5}{2}^-$ level, the number of counts used in the simulation of Fig. 6 are multiplied by a factor of 1.16 to correct for finite counting time and dead time, and then divided by 6116, the number of implanted ${}^9\text{C}$ ions. We have estimated the error in the resulting branching ratio based upon uncertainties in the subtraction of the simulated beta energy-loss spectrum. The branching ratio to the

TABLE II. Observed excitation energies, widths, and nucleon decay branching ratios to the ground state of ${}^8\text{Be}$ for the first three negative parity levels in ${}^9\text{Be}$ and ${}^9\text{B}$.

J^π	Nucleus	E_x (MeV)	Γ (keV)	Fraction of decays to ${}^8\text{Be}_{\text{g.s.}}$ + nucleon (%)	Reference
$\frac{3}{2}^-$	${}^9\text{Be}$	0.00	stable		
$\frac{3}{2}^-$	${}^9\text{B}$	0.00	0.5 ± 0.02		Teranishi and Furubayashi (Ref. 15)
$\frac{5}{2}^-$	${}^9\text{Be}$	2.43	0.77 ± 0.15		Ajzenberg-Selove (Ref. 6)
$\frac{5}{2}^-$	${}^9\text{Be}$			≤ 10	Bodanski <i>et al.</i> (Ref. 59)
$\frac{5}{2}^-$	${}^9\text{Be}$			13 ± 3.0	Mösner <i>et al.</i> (Ref. 22)
$\frac{5}{2}^-$	${}^9\text{Be}$			7.5 ± 1.5	Christensen and Cocke (Ref. 60)
$\frac{5}{2}^-$	${}^9\text{Be}$			6.4 ± 0.12	Chen <i>et al.</i> (Ref. 8)
$\frac{5}{2}^-$	${}^9\text{B}$	2.36	81 ± 5		Ajzenberg-Selove (Ref. 6)
$\frac{5}{2}^-$	${}^9\text{B}$			≤ 1.0	Wilkinson <i>et al.</i> (Ref. 7)
$\frac{1}{2}^-$	${}^9\text{Be}$	3.0 ± 0.1	1000 ± 200	(100) ^a	Macefield <i>et al.</i> (Ref. 21)
$\frac{1}{2}^-$	${}^9\text{Be}$	2.78 ± 0.12	1100 ± 120	(100) ^a	Chen <i>et al.</i> (Ref. 8)
$\frac{1}{2}^-$	${}^9\text{Be}$	2.9 ± 0.25	1000 ± 250	≥ 72	Adloff <i>et al.</i> (Ref. 54)
$\frac{1}{2}^-$	${}^9\text{Be}$			≈ 30	Langevin <i>et al.</i> (Ref. 27)
$\frac{1}{2}^-$	${}^9\text{B}$	2.6 ± 0.1	1650 ± 100		Fazely <i>et al.</i> (Ref. 32)
$\frac{1}{2}^-$	${}^9\text{B}$	2.75 ± 0.3	3130 ± 200		Pugh (Ref. 33)

^aThese values have not been measured. They are assumptions used in each of these references for the analysis of the beta-delayed neutron spectra. See Sec. IV.

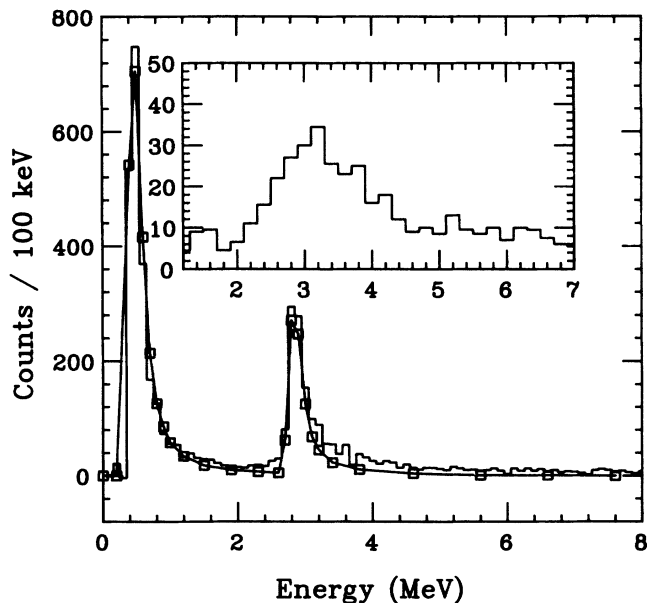


FIG. 5. The ${}^9\text{C}$ decay data recorded in E1 is shown in the figure as a histogram, and a simulated line shape for the ground state and narrow $\frac{5}{2}^-$ level is illustrated by the squares and solid line. Squares have been omitted from regions where the simulation is smooth. The simulation is subtracted from the data, and the difference is shown in the inset, where two channel averages are given.

$\frac{1}{2}^-$ level is found by scaling the branching ratio of the $\frac{5}{2}^-$ by a factor of $1/(1.5 \pm 0.5)$. The ground state branch is obtained in a similar manner to that of the $\frac{5}{2}^-$ level, except that an additional 14% is added to the resulting branching ratio to account for the less-than-unity efficiency of the constant fraction discriminator for the lowest amplitude pulses detected. The results are given in Table I. The beta-decay $B(\text{GT})$ values given in Table

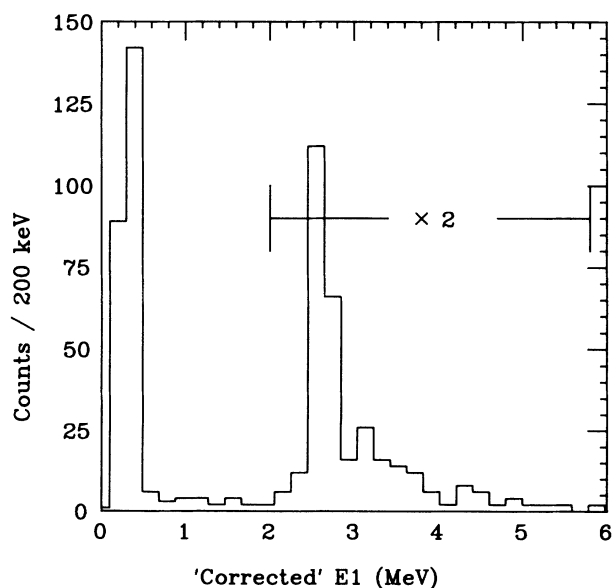


FIG. 6. The decay energy in E1 corrected for the β energy loss as described in the text. The data above 2.0 MeV have been multiplied by a factor of 2.

I are calculated using the following expressions:

$$ft = \frac{f(Q_B - E_x)t_{1/2}}{\text{branching ratio}} \quad (3)$$

and

$$B(\text{GT}) = \frac{6177 \text{ s}}{ft} \quad (4)$$

The statistical rate function $f(Q_B - E_x)$ is calculated using the method of Wilkinson and Macefield.¹⁶ No adjustments have been made for the widths of the states; the $\frac{1}{2}^-$ was treated as a narrow state at 2.9 MeV.

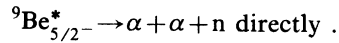
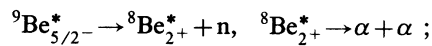
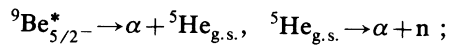
A peak near 12 MeV excitation in ${}^9\text{B}$ is evident in the spectra from both E1 (Fig. 3) and E2 (not shown). In contrast to the results of the delayed proton data,^{3,4} no peak is observed near 9 MeV. The peak near 12 MeV in the present data is best described as a branch to a level with $E_x = 12.1 \pm 0.6$ MeV with a width of 400 ± 100 keV after broadening due to beta energy loss and resolution has been taken into account. The area under the peak within 800 keV of E_x represents $2.3 \pm 0.5\%$ of the decay strength. The actual branch to this state may be larger, because additional strength to this state may be found far below the peak (i.e., up to ~ 25 FWHM units) in the present spectrum. This can be the result of two separate effects: one experimental—the escape of the highest-energy protons from the silicon; and one physical—a long low energy tail of the peak which can be understood as the effect of the Fermi statistical rate function on the low energy part of the Breit-Wigner distribution used to describe the state.^{17,18} These effects depend greatly on the particle decay modes of the state, and will be dealt with in a forthcoming paper.¹⁹ Thus, the above estimate of the fraction of the decay strength is only an experimental lower limit.

IV. THE BETA DECAY OF THE MIRROR NUCLEUS ${}^9\text{Li}$

The beta decay branching ratios of ${}^9\text{Li}$ have been investigated by many groups, but the determination of the excitation spectrum in ${}^9\text{Be}$ following the beta decay of ${}^9\text{Li}$ has been complicated by uncertainties in the decay modes of the excited states in ${}^9\text{Be}$. The particle decay of excited states of ${}^9\text{Be}$ always involves both charged and uncharged particles ($2\alpha + \text{neutron}$). These require very different equipment for detection. Experiments have either measured energy spectra of single alpha particles, alpha-alpha coincidences, or neutron time-of-flight spectra. To extract structure and branching ratio information, the measured spectra were fit with calculated functions based on some model for the particle decay. Previously determined beta-decay branching ratios of ${}^9\text{Li}$ have been summarized in Table I. We have calculated the corresponding $B(\text{GT})$ values from these branching ratios in the same way as for ${}^9\text{C}$ decay (see Sec. III). A value of 0.177 s is used for the half-life of ${}^9\text{Li}$.²⁰

Both Chen *et al.*⁸ and Macefield *et al.*²¹ have studied the beta-delayed neutron time-of-flight spectrum to determine the beta decay branching ratios of ${}^9\text{Li}$. Each group clearly identified three peaks in this spectrum.

They agree on the origin of each peak. The peak representing the highest energy neutrons was identified as the neutron decay of the broad $\frac{1}{2}^-$ state in ${}^9\text{Be}$ to the ground state of ${}^8\text{Be}$. The intermediate energy peak was attributed to the small neutron-decay branch of the $\frac{5}{2}^-$ state to the ground state of ${}^8\text{Be}$. The lowest energy peak was thought to result from the majority of the decays of the $\frac{5}{2}^-$ through broad intermediate states. This last particle decay branch, which resulted in neutrons with lower energy than the ${}^8\text{Be}_{\text{g.s.}} + n$ channel, could be attributed to any one or combination of the following decay channels:



Mösner *et al.*²² have pointed out that the calculated phase-space population of the two alpha particles is quite similar in these three channels. It is possible that some insight could be gained into the structure and breakup dynamics of this level (and other levels in mass 9) through the use of three-body nuclear models. Based on the Born-Oppenheimer model of the H_2^+ molecule, three-body $\alpha + \alpha + n$ calculations reproduce the level structure in ${}^9\text{Be}$.^{23,24} The beta-decay half-life of ${}^6\text{He}$ and the breakup of ${}^6\text{Li}^*$ through sequential decay channels have been predicted with a three-body $\alpha + N + N$ calculation based on separable two-body potentials.²⁵

In order to determine the absolute branching ratios, Chen *et al.*⁸ and Macefield *et al.*²¹ assume that all of the beta decay strength of ${}^9\text{Li}$ is to the first $\frac{3}{2}^-$, $\frac{5}{2}^-$, and $\frac{1}{2}^-$ levels. Further, they assume that the highest energy neutron group comes only from the decay of the $\frac{1}{2}^-$ level to the ground state of ${}^8\text{Be}$, and that the $\frac{1}{2}^-$ level can decay only in this manner. They also assume that the decay of the $\frac{5}{2}^-$ level to the ground state of ${}^8\text{Be}$ is the sole source of counts in the intermediate energy neutron group.

While the authors assume that the two highest energy neutron groups result from the decay of the $\frac{5}{2}^-$ and $\frac{1}{2}^-$ levels to the ground state of ${}^8\text{Be}$ only, they have used different values for the ground state beta decay branch, and different values for the fraction of the neutron decays of the $\frac{5}{2}^-$ state that lead to ${}^8\text{Be}_{\text{g.s.}}$. Chen *et al.*⁸ have determined the ${}^9\text{Li}$ ground state beta decay branching ratio to be 65% from a separate experiment, in which the beta-delayed 2α energy spectrum of ${}^9\text{Li}$ ions implanted in silicon was recorded. Macefield *et al.*²¹ used a previously determined value of 75% from the beta-particle energy spectrum from ${}^9\text{Li}$ decay. Since Macefield *et al.* have not determined the ground-state branch themselves, but have relied on other measurements, we have adjusted their values to accommodate the more recent measurements for the ground state branching ratio of 50% by Björnstad *et al.*²⁶ and

Langevin *et al.*²⁷ It is these adjusted values that are included in Table I.

Langevin *et al.*²⁷ determined the branching ratios of ${}^9\text{Li}$ to the excited states of ${}^9\text{Be}$ levels listed in Table I from the beta-delayed alpha-particle spectrum only. They allowed more freedom in the choice of the various particle decay branching ratios in their fit. Their beta-decay branching ratio measurements are also included in Table I, and their particle decay branching ratios are included in Table II.

All measurements of the fraction of the decays of the $\frac{5}{2}^-$ state in ${}^9\text{Be}$ that populate the ground state of ${}^8\text{Be}$ are in fairly good agreement, as shown in Table II. In a pure p -shell independent particle model this decay is explicitly forbidden, since it must proceed through nucleon decay with $l=2$. The description of this state must therefore include some admixture of higher orbitals. This issue has been addressed by Spencer *et al.*²⁸ and Henley and Kunz.²⁹ While Spencer *et al.*²⁸ only conclude that this fraction must be small, Henley and Kunz²⁹ predict that this value should lie between 5% and 20%, in agreement with the data. In the mirror system, the proton decay of the $\frac{5}{2}^-$ state in ${}^9\text{B}$ to the ground state of ${}^8\text{Be}$ has not been observed, and Wilkinson *et al.*⁷ have set an upper limit on the branching ratio of 1% for this decay. This large asymmetry in the observed branching ratios does not necessarily imply a difference in the nuclear structure aspect of the decay. The data on the decay of the state in ${}^9\text{Be}$ suggest a partial width for the decay to the ground state of ${}^8\text{Be}$ of less than a tenth of a keV. Since the $\frac{5}{2}^-$ level in ${}^9\text{B}$ has a width of roughly 80 keV (more than 100 times larger than the total width in ${}^9\text{Be}$), it appears that there is more phase space available for decays that do not lead to the ground state of ${}^9\text{Be}$. Nyman *et al.*¹⁷ have confirmed the narrowness of this level produced in the beta decay of ${}^9\text{Li}$, and in an elegant experiment, measured the broadening of the delayed neutron peak due to the recoil of the excited ${}^9\text{Be}$ after beta decay.

Both Nyman *et al.*¹⁷ and Langevin *et al.*²⁷ have found evidence for the population of at least one state near 12 MeV in ${}^9\text{Be}$ following the beta decay of ${}^9\text{Li}$. In both of these experiments and in the present ${}^9\text{C}$ decay data (see Sec. III), modeling of the particle decay modes plays a strong role in the extraction of a value for the $B(\text{GT})$ for this state. Because of this complication, we defer quantitative comparison between these measurements to a future work.¹⁹

Langevin *et al.*²⁷ have fit the high-energy portion of the beta-delayed alpha particle spectrum from the decay of ${}^9\text{Li}$ with a calculation of the statistical three-body breakup of a previously reported level at 11.28 MeV. The choice of this excitation energy was somewhat arbitrary, in that this value was not determined from the data. Instead, it was chosen from a list of known states in ${}^9\text{Be}$.⁶ In their analysis, sequential decay through excited states in ${}^8\text{Be}$ and the ground and excited states of ${}^5\text{Li}$ were ignored, and the strength at lower excitation energies due to the distortion of the line shape by the roughly $(Q_\beta - E_x)^5$ dependence of the statistical rate function was not included.^{17,18}

Once a fit was made to the calculated α particle spectrum of Langevin *et al.*,²⁷ based upon the statistical three-body decay of an undistorted level at 11.28 MeV, which was fitted to the recorded spectrum for the highest energy alpha particles and subtracted from the data, a small residual component remained. They have assigned these remaining counts to the beta decay of ${}^9\text{Li}$ to an additional, previously reported level in ${}^9\text{Be}$, followed by an unspecified decay mode. They have assigned a branching ratio of $1.5 \pm 0.5\%$ to a level at 7.94 MeV.

Following an analysis of the high-energy beta-delayed alpha particles from ${}^9\text{Li}$, Nyman *et al.*¹⁷ propose that two levels in ${}^9\text{Be}$ near 12 MeV (those listed in Ajzenberg-Selove⁶) are both populated, and that these levels decay through the ${}^5\text{He}_{g.s.} + \alpha$ channel. The effects of the penetrability of the alpha particle and the beta-decay phase-space factor are explicitly included in the fit. However, channels involving excited states of ${}^5\text{He}$ or ${}^8\text{Be}$, or direct three-body breakup, are ignored.

V. THE ${}^9\text{Be}(p,n){}^9\text{B}$ REACTION

Recently, there has been much effort to understand to what extent the (p,n) reaction cross section at small angles and high incident proton energies (> 100 MeV) is proportional to Gamow-Teller strength. Reviews of this relationship can be found by Goodman *et al.*³⁰ and Taddeucci *et al.*³¹ The Gamow-Teller component of the ${}^9\text{Be}(p,n){}^9\text{B}$ reaction can populate the same levels in ${}^9\text{B}$ as the beta decay of ${}^9\text{C}$. Since the initial state is now ${}^9\text{Be}$ instead of ${}^9\text{C}$, and there is no $\beta^+\nu$ phase-space weighting, the observed intensities will be very different than for the case of ${}^9\text{C}$ decay.

Fazely *et al.*³² and Pugh³³ report cross sections for the ${}^9\text{Be}(p,n){}^9\text{B}$ reaction, and Pugh describes a detailed analysis of the data. Cross sections for those levels which peak at 0° are listed in Table III, and the reported parameters which describe the broad $\frac{1}{2}^-$ level are included in Table II. While this work represents the

clearest indication of the broad $\frac{1}{2}^-$ level in ${}^9\text{B}$ besides the present ${}^9\text{C}$ decay data, there still remains a large uncertainty in the nature of this level. Fazely *et al.*³² show a fit to the neutron spectrum at a small angle using a level at 2.6 MeV with a width of 1.65 MeV. However, the more complete analysis of the data by Pugh³³ indicates a larger width of about 3 MeV for this 2.6 MeV state. The increase may be related to the introduction of a narrow $\frac{5}{2}^+$ level at 2.71 MeV in the fit. It is not clear if more levels are contributing to the spectrum. Since beta decay involves only Gamow-Teller transitions, it populates fewer states. Therefore, widths extracted from these experiments are likely to be more reliable than from the ${}^9\text{Be}(p,n){}^9\text{B}$ reaction.

We have estimated $B(\text{GT})$ values from the ${}^9\text{Be}(p,n){}^9\text{B}$ reaction cross sections, and include the results in Table III. These estimates are based on three simple assumptions: (1) the cross section at 0° is directly proportional to $B(\text{GT})$ (except between analog states where there is an additional Fermi component), (2) the $B(\text{GT})$ value for the ground-state to ground-state transition is 1.00 (a value close to the four theoretical values—see the following section), and (3) 15% of the cross section of the ground-state to ground-state analog transition is due to the Fermi component [based on the distorted wave impulse approximation (DWIA) calculations presented in Ref. 33]. We have chosen the ground-state transition $B(\text{GT})$ as the best reference for normalization. These assumptions give a proportionality constant such that for all nonanalog transitions,

$$B(\text{GT}) = 0.121\sigma(0^\circ), \quad (5)$$

where σ is in units of mb/sr. This value is in agreement with the more thorough treatment of this relationship by Goodman *et al.*³⁰ and Taddeucci *et al.*³¹

VI. SHELL MODEL CALCULATIONS

We have calculated the level schemes of the $A=9$ system within the full p -shell model space using the shell-

TABLE III. Excitation energies, widths, and cross sections of those levels reported by Pugh (Ref. 33) whose cross section peaks at 0° in the ${}^9\text{Be}(p,n){}^9\text{B}$ reaction. The $B(\text{GT})$ values are from Eq. (5).

E_x (MeV)	FWHM (MeV)	σ at 0.0° (mb/sr)	σ at 3.4° (mb/sr)	Deduced $B(\text{GT})$
0.00	a	9.52 ± 0.04	7.56 ± 0.06	(1.000) ^b
2.36	a	2.09 ± 0.04	1.68 ± 0.06	0.253
2.71 ± 0.1	0.71 ± 0.1	2.83 ± 0.36	2.10 ± 0.34	(0.342) ^c
2.75 ± 0.3	3.13 ± 0.2	9.73 ± 0.29	8.24 ± 0.26	1.177
4.3 ± 0.2	1.6 ± 0.2	2.41 ± 0.06	2.15 ± 0.06	0.292
12.23 ± 0.1	0.5 ± 0.1	0.230 ± 0.014	0.188 ± 0.017	0.028
13.96 ± 0.1	d	0.066 ± 0.002	0.049 ± 0.005	0.008
14.60 ± 0.1	0.6 ± 0.1	0.213 ± 0.025	0.173 ± 0.040	0.026

^aThe experimental widths of these peaks are used to define the experimental resolution (≈ 0.4 MeV FWHM).

^bThis value was fixed in order to find the proportionality constant in Eq. (5).

^cThe identity of this state is uncertain, but if it represents strength to a level separate from the broad $\frac{1}{2}^-$ at 2.75, it is not a $J^\pi = \frac{1}{2}^-$, $\frac{3}{2}^-$, or $\frac{5}{2}^-$ level, according to shell model predictions. This being the case, it would not be populated through the Gamow-Teller channel as discussed in the text, and thus a value for $B(\text{GT})$ would not be appropriate.

^dThe intrinsic width of the state could not be determined beyond the conclusion that it is small compared to the experimental resolution.

TABLE IV. Shell model predictions for the $A=9$ system. The beta-decay $B(\text{GT})$ values are for beta decay of ${}^9\text{C}$ or ${}^9\text{Li}$, to the J^π state predicted to lie at E_x , MeV in ${}^9\text{B}$ or ${}^9\text{Be}$. All values in square brackets refer to powers of ten (i.e., $8.0[E^* - 9] = 8.0 \times 10^{-9}$). The spectroscopic factors for the allowed particle decay modes for the pure p -shell model are listed, and the resulting width (keV) given in parentheses to the right of the corresponding spectroscopic factor. The widths are calculated from Eq. (6) in the text. Predictions for four interactions are given in the following order: Cohen and Kurath (6–16) 2BME (Ref. 35), Millener (Ref. 37), and Cohen and Kurath (8–16) POT (Ref. 35).

J^π	E_x (MeV)	β -decay $B(\text{GT})$	${}^9\text{Be}(p,n){}^9\text{B}$ $B(\text{GT})$	${}^8\text{Be}_{0^+} + p$ $l=1$	${}^8\text{Be}_{2^+} + p$ $l=1$	${}^5\text{Li}_{3/2^-} + \alpha$ $l=0$	${}^5\text{Li}_{3/2^-} + \alpha$ $l=2$	${}^5\text{Li}_{1/2^-} + \alpha$ $l=0$	${}^5\text{Li}_{1/2^-} + \alpha$ $l=2$	Total width (keV)
$\frac{3}{2}^-$	0.00	0.035	1.042	0.58 (2.1)	0.73	Group (a) 0.57	0.56	0.062	0.062	2.1
	0.00	0.046	0.994	0.57 (2.1)	0.75	0.55	0.58	0.048	0.048	2.1
	0.00	0.014	0.917	0.56 (2.0)	0.75	0.55	0.60	0.042	0.042	2.0
	0.00	0.086	0.972	0.57 (2.1)	0.78	0.55	0.56	0.054	0.054	2.1
	2.64	0.030	0.233		1.15		0.98	0.14	0.14	
	3.03	0.028	0.285		1.13		0.99	0.13	0.13	
	2.43	0.066	0.234		1.12		0.95	0.10	0.10	
	2.95	0.039	0.291		1.16		0.98	0.19	0.19	
	3.02	0.016	1.056	0.72 (4400)	0.46		0.57	0.65		4400
	2.75	0.020	1.052	0.72 (4400)	0.47		0.57	0.65		4400
$\frac{5}{2}^-$	3.25	0.010	1.049	0.75 (4600)	0.42		0.55	0.63		4600
	1.79	0.080	1.028	0.77 (4700)	0.41		0.54	0.61		4700
	5.09	0.005	0.391	0.049 (530)	1.15 (5000)	Group (b) 0.069 (360)	0.31 (780)	0.81	0.81	6700
	4.87	0.069	0.470	0.064 (690)	1.13 (4900)	0.092 (490)	0.26 (660)	0.84	0.84	6700
	5.49	0.014	0.488	0.053 (570)	1.13 (4900)	0.077 (410)	0.27 (680)	0.78	0.78	6600
	4.66	0.081	0.484	0.041 (440)	1.14 (5000)	0.082 (430)	0.26 (660)	0.79	0.79	6500
	7.48	0.140	0.011		0.40 (3900)		0.0087 (49)	0.32	0.32	3900
	7.66	0.004	0.021		0.42 (4100)		0.0028 (16)	0.35	0.35	4100
	6.91	0.010	0.038		0.49 (4800)		0.0083 (47)	0.36	0.36	4800
	7.39	0.032	0.005		0.38 (3700)		0.0007 (4)	0.28	0.28	3700
$\frac{3}{2}^-$	9.93	1.88	0.062	0.0018 (38)	0.0013 (23)	Group (c) 0.0041 (49)	0.010 (100)	0.0003 (0.8)	0.0003 (0.8)	210
	9.35	1.42	0.016	8.0[E-9] (0)	0.016 (280)	0.0007 (8)	0.028 (280)	0.018 (46)	0.018 (46)	610
	9.98	1.45	0.022	0.0016 (34)	0.0011 (19)	0.0029 (35)	0.0075 (75)	0.0003 (0.8)	0.0003 (0.8)	160
	10.04	1.78	0.080	1.7[E-7] (0)	0.015 (260)	0.0013 (16)	0.039 (390)	0.022 (56)	0.022 (56)	730
	11.50	0.10	0.049	0.0076 (160)	0.0073 (130)		0.0051 (51)	0.0058 (31)	0.0058 (31)	370
	9.70	0.38	0.022	0.0007 (15)	0.0036 (63)		0.0020 (20)	0.0023 (12)	0.0023 (12)	110
	8.10	0.45	0.025	0.0056 (120)	1.4[E-4] (2)		0.0065 (65)	0.0074 (39)	0.0074 (39)	230
	11.02	0.25	0.038	0.0010 (21)	0.0052 (91)		0.0014 (14)	0.0016 (8)	0.0016 (8)	130

TABLE IV. (Continued).

J^π	E_x (MeV)	β -decay $B(\text{GT})$	${}^9\text{Be}(\text{p,n}){}^9\text{B}$ $B(\text{GT})$	${}^8\text{Be}_{0^+} + \text{p}$ $l=1$	${}^8\text{Be}_{2^+} + \text{p}$ $l=1$	${}^5\text{Li}_{3/2^-} + \alpha$ $l=0$	${}^5\text{Li}_{3/2^-} + \alpha$ $l=2$	${}^5\text{Li}_{1/2^-} + \alpha$ $l=0$	${}^5\text{Li}_{1/2^-} + \alpha$ $l=2$	Total width (keV)
$\frac{5}{2}^-$	11.61	2.32	0.024	0.028 (490)	0.0079 (79)		0.0079 (79)	0.029 (74)	0.029 (74)	640
	9.80	2.48	0.000	0.0037 (65)	0.010 (100)		0.010 (100)	0.0048 (12)	0.0048 (12)	180
	10.13	1.89	0.046	0.019 (330)	0.029 (290)		0.029 (290)	0.020 (51)	0.020 (51)	670
$\frac{1}{2}^-$	10.87	2.66	0.000	0.0058 (100)	0.0038 (38)		0.0038 (38)		0.0089 (23)	160
	12.18	1.63	0.000	0.0005 (11)	0.0004 (7)		0.0032 (32)	0.0037 (20)		70
	13.03 ^a	1.00	0.002	0.0014 (30)	0.006 (110)		0.011 (110)	0.012 (64)		310
	13.34 ^b	1.19	0.019	3.3[E-5] (0.7)	0.0030 (52)		4.0[E-5] (0.4)	5.0[E-5] (0.3)		53
	12.04	1.42	0.017	0.0039 (82)	0.019 (330)		0.024 (240)	0.038 (200)		850

^aBelow this state the Millener (Ref. 36) interaction also predicts states at 11.98 MeV ($\frac{5}{2}^-$) and 12.40 MeV ($\frac{3}{2}^-$).

^bBelow this state the Kumar (Ref. 37) interaction also predicts states at 11.36 MeV ($\frac{5}{2}^-$), 12.04 MeV ($\frac{3}{2}^-$), and 12.24 MeV ($\frac{3}{2}^-$).

model code OXBASH.³⁴ Four interactions were considered, two of the original interactions of Cohen and Kurath,³⁵ i.e., the (6–16) 2BME and the (8–16) POT interactions, as well as the more recent interactions of Millener³⁶ and Kumar.³⁷ All of these are based upon a least-squares fit of the interaction parameters to some subset of the p -shell binding energies and energy levels.

Predicted excitation energies of $\frac{1}{2}^-$, $\frac{3}{2}^-$, and $\frac{5}{2}^-$ levels in ${}^9\text{B}$ and ${}^9\text{Be}$, and $B(\text{GT})$ values for the population of these levels from the beta decay of ${}^9\text{C}$ and ${}^9\text{Li}$, and from the ${}^9\text{Be}(\text{p,n}){}^9\text{B}$ reaction are summarized in Tables IV and III, respectively. These theoretical $B(\text{GT})$ values are defined in Ref. 38 and include the $(g_A/g_V)^2$ factor. They have also been multiplied by a factor of 0.6 to take into account the empirical quenching observed for this operator.³⁸ Since binding energy and isospin mixing corrections have not been considered, the predicted excitation energies and beta-decay $B(\text{GT})$ values apply to both members of the mirror system.

Table IV contains calculated spectroscopic factors for all available two-body decay channels using each of the four p -shell interactions. Channels for which there can be no strength from a pure p -shell model have blank entries. The α -particle spectroscopic amplitudes were calculated using an SU(3) cluster for the α particle as described in Ref. 39, and were cross-checked against similar calculations provided by Millener.⁴⁰ We have calculated the partial widths based on the decay of these levels in ${}^9\text{B}$. The resulting widths in keV are listed in parentheses to the right of the corresponding spectroscopic factors in Table IV. The widths are given by^{41–44}

$$\Gamma_l = 2\theta_l^2 \gamma^2 P_l(E_x - Q), \quad (6)$$

where θ_l^2 is the spectroscopic factor, P_l is the penetrability, E_x is the excitation energy of the ${}^9\text{B}$ nucleus, and γ^2 is the Wigner single particle reduced width given by

$$\gamma^2 = \frac{3}{2} \frac{(\hbar c)^2}{\mu R_0^2}. \quad (7)$$

Here μ is the reduced mass. The penetrabilities were calculated from the Coulomb wave functions using the method of Steed as described by Barnett.⁴⁵

The channel radius R_0 was set to 4.0 fm for the ${}^8\text{Be} + \text{p}$ channels, and 4.5 fm for the ${}^5\text{Li} + \alpha$ channels. The penetrabilities for the first three levels are calculated using the excitation energies of 0.00, 2.36, and 2.9 MeV, for the $\frac{3}{2}^-$, $\frac{5}{2}^-$, and $\frac{1}{2}^-$ levels, respectively. For the next two levels, the theoretical excitation energies for each prediction are used. All of the penetrabilities for the last four levels predicted to lie above 8 MeV are calculated, assuming the state is at an excitation energy of 12.1 MeV. Where calculated, the penetrabilities for the ${}^8\text{Be}_{\text{g.s.}} + \text{p}$, ${}^8\text{Be}_{2^+} + \text{p}$, ${}^5\text{Li}_{\text{g.s.}} + \alpha$, and ${}^5\text{Li}_{1/2^-} + \alpha$ channels are calculated, assuming $Q = -0.19, 2.7, 1.69$, and 8.69 MeV, respectively. The last three values represent arbitrary effective centroids for the broad intermediate states in ${}^8\text{Be}$ and ${}^5\text{Li}$.

For states above the Coulomb plus centrifugal barrier, which lies a few MeV above threshold for p and α emission from light nuclei, the penetrability represents

roughly the available phase space (e.g., $k^2 dk \approx k dE \approx \sqrt{E} dE$, where k and E are the center-of-mass momentum and energy for the decay). Thus for a given spectroscopic factor, the widths of the states are only slowly varying functions of the actual binding energy of the state. Therefore, once above the Coulomb barrier, the widths for the mirror decays to ${}^8\text{Be} + p$ or n should be similar to each other, as should those for $\alpha + {}^5\text{Li}$ or ${}^5\text{He}$. Given the uncertainty in the calculated spectroscopic factors, it is not important at the moment to include the small differences between these unbound levels in mirror nuclei. Thus, the widths given for states above 4 MeV in ${}^9\text{B}$ can be treated as estimates of the widths of the same levels in ${}^9\text{Be}$.

The major uncertainties in these width calculations are related to the approximations used in Eq. (6), and to the fact that the small spectroscopic factors will be sensitive to admixtures from configurations outside the p -shell model space. We believe that the former is responsible for the "factor of 4" discrepancy discussed in the following section. Equation (6) could be replaced with more complete models;⁴⁶ however, this treatment would be beyond the scope of the present work.

VII. DISCUSSION

The states in Table IV can be divided into three groups: (a) the lowest three states below 4 MeV which have small beta-decay $B(\text{GT})$ values but which dominate in the beta decay of ${}^9\text{C}$ and ${}^9\text{Li}$ because of the large Q value for the decay; (b) the next two states lying between 4 and 8 MeV which also have small beta-decay $B(\text{GT})$ values; and (c) the next few states above 8 MeV which have large beta-decay $B(\text{GT})$ values. We will use this division to organize our discussion.

A. Group (a): States below 4 MeV

The states in group (a) have small $B(\text{GT})$ values for beta decay; that is, small compared to the sum-rule value of $0.6(g_A/g_V)^2 3(Z-N) = 8.5$. For these states, the original (6-16) 2BME interaction of Cohen and Kurath³⁵ appears to give the best overall agreement with experiment for both energy levels and beta decay $B(\text{GT})$ values. Indeed, these $B(\text{GT})$ values are in remarkably good agreement given the smallness of the values (see Table I). The states in group (a) have large spectroscopic factors for the allowed nucleon decays to the ground state and 2^+ states of ${}^8\text{Be}$, and allowed α decays to the ground state of ${}^5\text{Li}$ (see Table IV). The calculated $B(\text{GT})$ values for the ${}^9\text{Be}(p,n){}^9\text{B}$ reaction of Table IV also agree well with the experimental values of Table III.

While the two most recent measurements of the branching ratio for the ${}^9\text{Li} \rightarrow {}^9\text{Be}$ ground state beta decay yield $B(\text{GT})$ which agree favorably with the value for ${}^9\text{C}$ decay (see Table I), agreement between measurements for decays to the other two low-lying states is not as good. In the case of the $\frac{1}{2}^-$ level, the values for the ${}^9\text{Li}$ decay span a range of a factor of 5, with our value from ${}^9\text{C}$ decay close to the middle. In the case of the branch

to the $\frac{5}{2}^-$ level, the three $B(\text{GT})$ values for ${}^9\text{Li}$ decay are all very close, while our value for the decay of ${}^9\text{C}$ is lower than these values by more than a factor of 2. If isospin is conserved, the wave functions for mirror levels, and thus the $B(\text{GT})$ values for mirror beta decays, should be identical. Deviations from mirror symmetry have been extensively investigated, and examples of asymmetry in beta decay have been identified.^{47,48}

We define an asymmetry parameter,

$$\Delta = \sqrt{B(\text{GT})_-} - \sqrt{B(\text{GT})_+}, \quad (8)$$

as a way to express the absolute difference in the beta decay matrix elements. Previously the two largest absolute asymmetries observed in the p shell were found in the decays of ${}^{12}\text{B}$ and ${}^{12}\text{N}$ to the ground state of ${}^{12}\text{C}$ ($\Delta = 0.043$),⁴⁹ and the decays of ${}^{13}\text{B}$ and ${}^{13}\text{O}$ in the ground states of ${}^{13}\text{C}$ and ${}^{13}\text{N}$, respectively ($\Delta = 0.076$).⁵⁰⁻⁵² As given, the data in Table I suggest a value $\Delta = 0.09 \pm 0.03$ for the decay to the $\frac{5}{2}^-$ level. Towner⁵³ has demonstrated that most of the measured asymmetries can be fairly well accounted for by small differences in the radial wave functions of the mirror states. This difference is due to the Coulomb interaction, which introduces an asymmetry in the binding energies of the mirror nuclei. However, for the decay to the $\frac{5}{2}^-$ level in mass 9, Towner predicts a value for Δ of only 0.008, an order of magnitude smaller than observed.

Inconsistencies between the various measurements of $B(\text{GT})$ values for ${}^9\text{Li}$ beta decay shown in Table I and particle decay branching ratios in Table II cast doubt on the branching ratio measurements for the decay of ${}^9\text{Li}$ to the $\frac{5}{2}^-$ level in ${}^9\text{Be}$. Each relies on some particular particle decay characteristic of the $\frac{5}{2}^-$ level that is not yet determined with suitable reliability. As an example, let us develop a possible explanation for the observed asymmetry between the $B(\text{GT})$ for the population of the $\frac{5}{2}^-$ level from ${}^9\text{Li}$ and ${}^9\text{C}$ decay, based on a misinterpretation of the beta-delayed particle spectra for ${}^9\text{Li}$.

The shell model calculations shown in Table IV indicate that the $\frac{1}{2}^-$ level in ${}^9\text{Be}$ and ${}^9\text{B}$ has a large spectroscopic factor for the decay into both the ground state and first excited state of ${}^8\text{Be}$. If the high-energy tail of this broad level neutron decays through the low energy tail of ${}^8\text{Be}_{2^+}^*$, these events could contaminate the intermediate energy peak in the delayed neutron spectrum discussed in Sec. IV, and as a result cause the branching ratio to the $\frac{5}{2}^-$ level to be overestimated.

In order to be more quantitative, let us assume that the beta decay branching ratios of ${}^9\text{Li}$ to the $\frac{5}{2}^-$ and $\frac{1}{2}^-$ levels of ${}^9\text{Be}$ are both 15%. We will use 7% as the fraction of the decays of the narrow $\frac{5}{2}^-$ level to the ground state of ${}^8\text{Be}$ (consistent with previous experiments; see Table II). If 5% of the decays of the $\frac{1}{2}^-$ state populate the first 2^+ state of ${}^8\text{Be}$ instead of the ground state, and these lower energy neutrons are mistaken as neutrons from the decay of the $\frac{5}{2}^-$ level to the ground state of ${}^8\text{Be}$, the inferred branching ratio to the $\frac{1}{2}^-$ level will be reduced slightly to about 14%. However, since the strength of the intermediate energy neutron group must

be multiplied by $1/0.07=14.3$ in order to obtain the branching ratio to the $\frac{5}{2}^-$ level, the inferred branching ratio to this state will be

$$14.3 \times [(15\% \times 0.07) + (15\% \times 0.05)] = 26\% \quad (9)$$

instead of 15%. Here, the first term represents the real branch to the $\frac{5}{2}^-$ level, and the second term represents the branch to the $\frac{1}{2}^-$ level that would be mistaken as additional population of the $\frac{5}{2}^-$ level.

While only an instructive example, this scenario is consistent with the known data. Adloff *et al.*⁵⁴ have given only an upper limit of 28% to the fraction of the decays of the $\frac{1}{2}^-$ level that do not decay to the ground state of ${}^8\text{Be}$. (Langevin *et al.*²⁷ suggest a value for this fraction of 70%. However, this value is based in part on the branching ratio to the $\frac{1}{2}^-$ level of Chen *et al.*,⁸ itself a factor of 5 lower than that of Macefield *et al.*²¹) The results listed in Table IV indicate a large spectroscopic factor for the decay of the $\frac{1}{2}^-$ level to the first excited state of ${}^8\text{Be}$, and so one must expect some fraction of the decays of the high-energy part of the broad $\frac{1}{2}^-$ level to decay through this channel, despite the Coulomb plus $l=1$ centrifugal barrier.

A possible candidate for a fourth level belonging to group (a) has been reported by Esterl *et al.*⁴ They observed a delayed proton group from the decay of ${}^9\text{C}$ that would correspond to a state in ${}^9\text{B}$ at 3.25 ± 0.25 MeV with a width of 0.2 ± 0.1 MeV, decaying by proton emission to the ground state of ${}^8\text{Be}$. The narrow width of this peak precludes the assignment to the first $\frac{1}{2}^-$ level discussed above. Based on the nonobservation of the population of this narrow state in our data, we put an upper limit on the value of the ${}^9\text{C}$ beta decay $B(\text{GT})$ value of 0.004 [or a $\log(ft) \geq 6.2$]. It is difficult to tell whether or not the peak of Esterl *et al.* is consistent with this strength. The shell model calculations (see Table IV) do not leave room for any narrow $\frac{1}{2}^-$, $\frac{3}{2}^-$, or $\frac{5}{2}^-$ levels between the first $\frac{5}{2}^-$ level at 2.36 and the levels of group (c) predicted to lie above 9 MeV. This peak cannot be attributed to the nucleon decay of a level near 6 MeV to the first 2^+ state of ${}^8\text{Be}$, since this state in ${}^8\text{Be}$ has a width of about 1.5 MeV, and the experimental peak has a width of only a fraction of an MeV. Thus, if this peak represents a state in ${}^9\text{B}$, it most likely represents a first-forbidden transition to a level near 3.25 MeV with a width of 0.2 ± 0.1 MeV.

B. Group (b): States between 4 and 8 MeV

We cannot identify any of the states in group (b) in the present experiment. This again is consistent with the shell-model calculations, which predict a small $B(\text{GT})$ value for the population of these states from beta decay. Both states in this group have strong spectroscopic factors for decay through the ${}^8\text{Be}_{2^+}^* + \text{nucleon}$ channel. While the $\frac{5}{2}^-$ level is predicted to decay nearly exclusively through this channel, the $\frac{3}{2}^-$ level is predicted

to have some strength to the ${}^8\text{Be}_{g.s.} + \text{nucleon}$ and mass $5 + \alpha$ channels.

Pugh³³ has identified a state in ${}^9\text{B}$ at 4.3 ± 0.2 MeV with a width of 1.6 ± 0.2 MeV, populated in the ${}^9\text{Be}(\text{p},\text{n}){}^9\text{B}$ reaction. The cross section for this level peaks at 0° , and implies a value for $B(\text{GT})$ of about 0.29 (see Table III and Sec. V). This represents an excellent match for the $\frac{3}{2}^-$ state of group (b) predicted to lie near 5 MeV. The predicted widths of the $\frac{3}{2}^-$ and $\frac{1}{2}^-$ levels of group (a) are both about a factor of 4 greater than observed in ${}^9\text{B}$ (compare values for these widths given in Tables II and IV). If the predicted width of the $\frac{3}{2}^-$ level of group (b) is similarly reduced by a factor of 4, the agreement between the calculated position and width of this level and the level described by Pugh³³ is nearly perfect. Esterl *et al.*⁴ have identified a peak in the delayed proton spectrum that could represent the proton decay of a level in ${}^9\text{B}$ at 4.0 ± 0.3 MeV with a width of 1.0 ± 0.2 MeV to the ground state of ${}^8\text{Be}$. From the calculated partial widths listed in Table IV, we estimate that the $\frac{3}{2}^-$ level of group (b) will decay through this channel roughly 10% of the time. It is then reasonable to suspect that beta decay to this $\frac{3}{2}^-$ level followed by proton decay to the ground state of ${}^8\text{Be}$ may be the source of the proton peak described by Esterl *et al.*⁴

The population of this $\frac{3}{2}^-$ level from the decay of ${}^9\text{C}$ would be difficult to observe in our present data, due to its large width. However, if present, it would manifest itself as a broad peak to the higher energy side of the peak due to the $\frac{1}{2}^-$ level in Fig. 5. The lack of observation of such a structure in the present data sets an upper limit for the $B(\text{GT})$ of 0.007 [$\log(ft)=5.9$] for the beta decay strength to the state reported by Pugh.³³ This is consistent with the small predicted $B(\text{GT})$ values for the $\frac{3}{2}^-$ state of group (b) listed in Table IV.

The $\frac{5}{2}^-$ level near 7 MeV is predicted to decay almost exclusively through the ${}^8\text{Be}_{2^+}^* + \text{nucleon}$. If we assume that the width is overpredicted by the same factor of 4 as discussed above, the width of this state is expected to be near 1 MeV. This level has small $B(\text{GT})$ values for population through both beta decay and the ${}^9\text{Be}(\text{p},\text{n})$ reaction. There is no evidence for such a level in the analysis of Pugh.³³ The same delayed proton peak of Esterl *et al.*⁴ that we have associated with the $\frac{3}{2}^-$ level of group (b) (see above) cannot be attributed to the decay of the $\frac{5}{2}^-$ level to the first 2^+ state of ${}^8\text{Be}$. This level is expected to have a width of at least 1 MeV, and the 2^+ state in ${}^8\text{Be}$ has a width of about 1.5 MeV. These two factors suggest that a delayed proton peak from this level should have a width in the lab of 2 MeV or more, in contrast to the observed width of 1.0 MeV observed by Esterl *et al.*⁴

Langevin *et al.*²⁷ observe a beta-decay branch of ${}^9\text{Li}$ to a broad level near 8 MeV. They have associated this strength with a reported level at 7.94 MeV in ${}^9\text{Be}$ (see Sec. IV). While this assignment is somewhat uncertain, their measured branching ratio of $1.5 \pm 0.5\%$ implies a $B(\text{GT})$ of 0.06 ± 0.02 [$\log(ft) \approx 5.0 \pm 0.1$] at this energy. This value is consistent with the predicted $B(\text{GT})$ for the $\frac{5}{2}^-$ level of group (b).

C. Group (c): States above 8 MeV

All of the states in group (c) have large $B(\text{GT})$ values for population by beta decay, and small $B(\text{GT})$ for the ${}^9\text{Be}(\text{p},\text{n})$ reaction. They all have very small spectroscopic factors for all of the decay channels considered in Table IV. Because of their small predicted widths, they are all candidates for the sharp state we observe near 12 MeV. For all of the interactions the predicted excitation energies are too low by 2–3 MeV. However, this is not an uncommon problem with shell model calculations. We note that all of the calculations also underpredict the excitation energy of the lowest $\frac{3}{2}^-$ $T=\frac{3}{2}$ state, which lies experimentally at 14.7 MeV, by amounts of 1.39, 2.26, 2.41, and 1.05 MeV, for the (6–16) 2BME,³⁵ Millener,³⁶ Kumar,³⁷ and (8–16) POT (Ref. 35) interactions, respectively (this is the same ordering as in Tables I and IV).

Pugh³³ has reported three states that are candidates for these four predicted levels. All of the predicted and experimental $B(\text{GT})$ values for the ${}^9\text{Be}(\text{p},\text{n}){}^9\text{B}$ reaction are so small that their uncertainties allow for no unambiguous assignments of any one of the predicted levels to any one measured level.

Hardy *et al.*³ and Esterl *et al.*⁴ report peaks in the delayed proton spectrum near 9 MeV and 12 MeV in the center of mass. There are at least three different explanations for these peaks; that the decay of ${}^9\text{C}$ populates

(1) two levels in ${}^9\text{B}$, the first level near 9 MeV with a width of 1.5 MeV, and the second is near 12 MeV with a width of 0.5 MeV—both levels at least occasionally proton decay to the ground state of ${}^8\text{Be}$;

(2) two levels in ${}^9\text{B}$ near 12 MeV populated in the ratio of 1.5:1, the first level decaying to the 2^+ excited state of ${}^8\text{Be}$, and the second level to the ground state;

(3) a single level in ${}^9\text{B}$ near 12 MeV, which proton decays to the broad 2^+ level in ${}^8\text{Be}$ at 3 MeV and to the ground state in the ratio of 1.5:1.

In all cases, the large continuum rising to the lower energy side of the two peaks can still be explained as the dominant decay of one (or both) level(s) through the ${}^5\text{Li}_{\text{g.s.}}+\alpha$ channel, generating protons with energies lower than those from the ${}^8\text{Be}$ channels. This is the only decay mode observed by Nyman *et al.*¹⁷ of one or more levels near 12 MeV in ${}^9\text{Be}$ populated from the beta decay of ${}^9\text{Li}$.

In the present experiment, we observe only a narrow peak near 12 MeV and do not observe the broad 9 MeV peak. We therefore can rule out (1). In order for (2) to be consistent with the single narrow peak in our data, the two levels should have nearly identical excitation energies or very different beta-decay branching ratios. Explanation (3) seems the simplest way to explain the two sets of data, and we will adopt this.

In Sec. III we determined the single standard deviation lower limit of the branching ratio to the narrow level at 12.1 ± 0.6 MeV as 1.8%. This value represents a value for the $B(\text{GT})$ of 0.6. The largest contribution to the uncertainty (and thus contributing to the smallness

of the lower limit) results from the uncertainty in the measured excitation energy of the state in our experiment. If the state can be assigned the same excitation as that of Esterl *et al.*,⁴ at 12.11 ± 0.10 MeV, then the one standard deviation lower limit for the $B(\text{GT})$ becomes 1.1. Corrections for efficiency will further increase these lower limits for the $B(\text{GT})$.

Of the predicted levels in group (c), only the $\frac{3}{2}^-$, $\frac{5}{2}^-$, and second $\frac{1}{2}^-$ levels have predicted beta decay $B(\text{GT})$ values large enough to be consistent with the measured $B(\text{GT})$. If we assume that there is only one level near 12 MeV that is strongly populated by beta decay, and that it is responsible for both peaks in the delayed proton data, then we must rule out the predicted $\frac{5}{2}^-$ level, since it should have no significant branch to the ground state of ${}^8\text{Be}$. This leaves us with only the $\frac{3}{2}^-$ and second $\frac{1}{2}^-$ levels of group (c) as candidates for the level populated by beta decay. If the underprediction of the excitation energies of these levels (as discussed in the beginning of this section) is taken into account, the agreement between the $\frac{3}{2}^-$ and the observed level at 12 MeV is complete, and the second $\frac{1}{2}^-$ level is too high by 2–3 MeV. While we cannot associate with certainty the 12.2 ± 0.1 MeV level observed by Pugh³³ with the level observed in beta decay, the observed strength in the ${}^9\text{Be}(\text{p},\text{n}){}^9\text{B}$ reaction is consistent with the predicted value for the $\frac{3}{2}^-$ level.

The level populated strongly near 12 MeV is clearly a part of the giant Gamow-Teller resonance. If indeed it turns out to be a $\frac{3}{2}^-$ level, this level might be described as the “antianalog” state. This term describes the level (or group of nearby levels) which have structure similar to that of the analog state itself, but have the isospin of the ground state. This strong transition can be compared to the strong beta decay of ${}^{12}\text{N}$ and ${}^{12}\text{B}$ to the 12.7 MeV $J^\pi=1^+$ $T=0$ level in ${}^{12}\text{C}$, with a $B(\text{GT})$ of about 2.0 [$\log(ft)\approx 3.5$].^{55,56} This level lies 2.4 MeV below the $J^\pi=1^+$, $T=1$ analog state in ${}^{12}\text{C}$. Assuming that our narrow state has a $J^\pi=\frac{3}{2}^-$, $T=\frac{1}{2}$ assignment, and that it is the level seen by Esterl *et al.*,⁴ at 12.1 MeV, the separation between this level and the analog $J^\pi=\frac{3}{2}^-$, $T=\frac{3}{2}$ level at 14.7 MeV in ${}^9\text{B}$ is 2.6 MeV. This is nearly the same separation as that between the $T=0$ and $T=1$ $J^\pi=1^+$ levels in ${}^{12}\text{C}$.⁶

VIII. SUMMARY

We have observed the population of the ground state and two low lying excited states in ${}^9\text{B}$ from the beta decay of ${}^9\text{C}$, by implanting the radioactive ions in solid state detectors. A technique was developed to remove the beta energy loss contamination of the spectrum, allowing for the use of much thicker detectors than has been previously possible. The branching ratios to these levels have been determined, and the results compared to several measurements of the decay of the mirror nucleus ${}^9\text{Li}$. We have also compared the beta decay data for both nuclei and the ${}^9\text{Be}(\text{p},\text{n}){}^9\text{B}$ cross sections to shell model predictions. The population of a state near 12 MeV from the decay of ${}^9\text{C}$ is confirmed, while a previ-

ously reported peak at 9 MeV in the delayed proton data is not seen. This supports the previous suggestion that the 9 MeV peak was generated by a state at 12 MeV decaying through the first excited state of ${}^8\text{Be}$.⁴

Overall, the agreement between the present data, the mirror decay of ${}^9\text{Li}$, the ${}^9\text{Be}(p,n){}^9\text{B}$ reaction, and shell model calculations is quite good. The most striking disagreement is between the mirror $B(\text{GT})$ values for ${}^9\text{C}$ and ${}^9\text{Li}$ decay to the lowest $\frac{5}{2}^-$ level in ${}^9\text{B}$ and ${}^9\text{Be}$, respectively. The three measurements for the ${}^9\text{Li}$ decay are all very close to each other, yet more than a factor of 2 greater than the value we observe for ${}^9\text{C}$ decay. We have suggested a possible systematic misinterpretation of the ${}^9\text{Li}$ decay data that might explain this observed asymmetry. The absolute difference between the observed matrix elements is ten times greater than predicted by Towner,⁵³ who is able to account for the asymmetries observed in other systems, and may be the largest observed to date.

There are many ambiguities that must be resolved before the level assignment and $B(\text{GT})$ strengths can be understood in mass 9. We feel that a new measurement of the beta decay of ${}^9\text{Li}$ is called for. The beta-delayed neu-

tron spectrum of ${}^9\text{Li}$ should be remeasured with the decay of the ${}^9\text{Li}$ nuclei occurring within a silicon detector or between a pair of silicon detectors. This would provide a highly efficient coincident detection of the delayed 2α energy. The complementary pair of excitation energy spectra in ${}^9\text{Be}$ and ${}^9\text{B}$ from the decay of ${}^9\text{Li}$ and ${}^9\text{C}$ will allow for a more complete characterization of the beta decay strengths in this system.

The reactions ${}^6\text{Li}({}^6\text{Li}, {}^3\text{H})$ and ${}^6\text{Li}({}^6\text{Li}, {}^3\text{He})$ may also be used to study the region near 12 MeV of excitation in ${}^9\text{B}$ and ${}^9\text{Be}$. These reactions have small calculated spectroscopic factors for the levels at low excitation, and large spectroscopic factors for states between 8 and 15 MeV of excitation in these nuclei.

ACKNOWLEDGMENTS

We would like to thank J. C. Hardy, D. J. Millener, and G. Bertsch for helpful comments on various subjects discussed in this paper. This work was supported in part by National Science Foundation Grant PHY 86-11210.

- ¹Joseph Cerny and J. C. Hardy, *Annu. Rev. Nucl. Sci.* **27**, 333 (1977).
- ²M. A. C. Hotchkis, J. E. Reiff, D. J. Vieira, F. Blönnigen, T. F. Lang, D. M. Moltz, X. Xu, and Joseph Cerny, *Phys. Rev. C* **35**, 315 (1987).
- ³J. C. Hardy, R. I. Verrall, R. Barton, and R. E. Bell, *Phys. Rev. Lett.* **14**, 376 (1965).
- ⁴John E. Esterl, David Allred, J. C. Hardy, R. G. Sextro, and Joseph Cerny, *Phys. Rev. C* **6**, 373 (1972).
- ⁵J. C. Hardy, private communication.
- ⁶F. Ajzenberg-Selove, *Nucl. Phys.* **A413**, 1 (1984).
- ⁷D. H. Wilkinson, J. T. Sample, and D. E. Alburger, *Phys. Rev.* **146**, 662 (1970).
- ⁸Y. S. Chen, T. A. Tombrello, and R. W. Kavanagh, *Nucl. Phys.* **146**, 136 (1970).
- ⁹C. A. Barnes and Davis B. Nichols, *Nucl. Phys.* **A217**, 125 (1973).
- ¹⁰Robert A. Langley, *Nucl. Instrum. Methods* **113**, 109 (1973).
- ¹¹K. Nichols and V. A. J. Van Lint, *Solid State Physics (Advances in Research and Applications)* (Academic, New York, 1966), Vol. 18, pp. 1–54.
- ¹²J. A. Nolen, Jr., L. H. Harwood, M. S. Curtin, E. Ormand, and S. Bricker, *Instrumentation for Heavy Ion Nuclear Research*, Proceedings of the International Conference on Instrumentation for Heavy Ion Research, Oak Ridge National Laboratory, Tennessee (Harwood Academic, New York, 1984).
- ¹³M. S. Curtin, L. H. Harwood, J. A. Nolen, B. Sherrill, Z. Q. Xie, and B. A. Brown, *Phys. Rev. Lett.* **56**, 34 (1986).
- ¹⁴J. M. Mosher, R. W. Kavanagh, and T. A. Tombrello, *Phys. Rev. C* **3**, 438 (1971).
- ¹⁵E. Teranishi and B. Furubayashi, *Phys. Lett.* **9**, 157 (1964).
- ¹⁶D. H. Wilkinson and B. E. F. Macefield, *Nucl. Phys.* **A232**, 58 (1974).
- ¹⁷G. Nyman, R. E. Azuma, B. Jonson, K.-L. Kratz, P. O. Larsson, S. Mattsson, and W. Ziegert, in Proceedings of the Fourth International Conference on Nuclei Far from Stability, Helsingør, 1981, edited by L. O. Skolen, Vol. I, p. 312.
- ¹⁸E. K. Warburton, *Phys. Rev. C* **33**, 303 (1986).
- ¹⁹D. Mikolas (unpublished).
- ²⁰E. Roeckl, P. F. Dittner, C. Détraz, R. Klapisch, C. Thibault, and C. Rigaud, *Phys. Rev. C* **10**, 1181 (1974).
- ²¹B. E. F. Macefield, B. Wakefield, and D. H. Wilkinson, *Nucl. Phys.* **A131**, 250 (1969).
- ²²Jürgen Mössner, Günter Schmidt, und Josef Schintlmeister, *Nucl. Phys.* **64**, 169 (1965).
- ²³A. C. Fonseca and P. E. Shanley, *Ann. Phys. (N.Y.)* **117**, 268 (1979).
- ²⁴A. C. Fonseca, J. Revai, and A. Matveenko, *Nucl. Phys.* **A326**, 182 (1979); J. Revai and A. V. Matveenko, *ibid.* **A339**, 448 (1980).
- ²⁵W. C. Parke, A. Ghovanlou, C. T. Noguchi, M. Rajan, and D. R. Lehman, *Phys. Lett.* **74B**, 158 (1978); W. C. Parke and D. R. Lehman, *Phys. Rev. C* **29**, 2319 (1984); **34**, E1496 (1986).
- ²⁶T. Björnstad, H. Å. Gustafsson, P. G. Hansen, B. Jonson, V. Lindfors, S. Mattsson, A. M. Poskanzer, and H. L. Ravn, *Nucl. Phys.* **A359**, 1 (1981).
- ²⁷M. Langevin, C. Détraz, D. Guillemaud, F. Naulin, M. Epherre, R. Klapisch, S. K. T. Mark, M. de Saint Simon, C. Thibault, and F. Touchard, *Nucl. Phys.* **A366**, 449 (1981).
- ²⁸R. R. Spencer, G. C. Phillips, and T. E. Young, *Nucl. Phys.* **21**, 310 (1960).
- ²⁹E. M. Henley and P. D. Kunz, *Phys. Rev.* **118**, 248 (1960).
- ³⁰C. D. Goodman, C. A. Goulding, M. B. Greenfield, J. Rapaport, D. E. Bainum, C. C. Foster, W. G. Love, and F. Petrovich, *Phys. Rev. Lett.* **44**, 1755 (1980).
- ³¹T. N. Taddeucci, C. A. Goulding, T. A. Carey, R. C. Byrd, C. D. Byrd, C. D. Goodman, C. Gaarde, J. Larsen, D. Horen, J. Rapaport, and E. Sugarbaker, *Nucl. Phys.* **A469**,

- 125 (1987), and E. Krofcheck, E. Sugarbaker, A. J. Wagner, J. Rapaport, D. Wang, J. N. Bahcall, R. C. Byrd, C. C. Foster, C. D. Goodman, C. Gaarde, D. J. Horen, T. Carey, and T. N. Taddeucci, *Phys. Lett.* **B189**, 299 (1987).
- ³²A. Fazely, B. Anderson, A. R. Baldwin, A. Kalenda, R. Madey, R. J. McCarthy, P. Tandy, J. Watson, W. Bertozzi, T. N. Buti, J. M. Finn, J. Kelly, M. A. Kovash, B. Pugh, and C. C. Foster, Indiana University Cyclotron Facility Annual Report, 1982, p. 49.
- ³³Billy Gene Pugh, Ph.D. thesis, Massachusetts Institute of Technology, 1985 (unpublished).
- ³⁴A. Etchegoyen, W. M. D. Rae, and B. A. Brown, Michigan State University Cyclotron Laboratory Report 524, 1985.
- ³⁵S. Cohen and D. Kurath, *Nucl. Phys.* **73**, 1 (1965).
- ³⁶D. J. Millener, private communication. This interaction is based on a fit of the two-body matrix elements to 48 levels in the mass region $A = 10-15$.
- ³⁷N. Kumar, *Nucl. Phys.* **A225**, 221 (1974).
- ³⁸B. A. Brown and B. H. Wildenthal, *At. Data Nucl. Data Tables* **33**, 347 (1985).
- ³⁹Munetake Ichimura, Akito Arima, E. C. Halbert, and Tokuo Terasawa, *Nucl. Phys.* **A204**, 225 (1973).
- ⁴⁰D. J. Millener, private communication.
- ⁴¹A. M. Lane and R. G. Thomas, *Rev. Mod. Phys.* **30**, 257 (1958).
- ⁴²J. B. French, in *Nuclear Spectroscopy*, edited by F. Ajzenberg-Selove (Academic, New York, 1960), p. 890.
- ⁴³M. H. Macfarlane and J. B. French, *Rev. Mod. Phys.* **32**, 567 (1960).
- ⁴⁴J. B. Marion and F. C. Young, *Nuclear Reaction Analysis* (North-Holland, Amsterdam, 1968), pp. 84-95 and 147.
- ⁴⁵A. R. Barnett, *Comput. Phys. Commun.* **27**, 147 (1982).
- ⁴⁶R. Sherr and G. Bertsch, *Phys. Rev. C* **32**, 1809 (1985).
- ⁴⁷D. H. Wilkinson, *Phys. Rev. Lett.* **27**, 1018 (1971).
- ⁴⁸D. H. Wilkinson, *Phys. Lett.* **48B**, 169 (1974).
- ⁴⁹D. E. Alburger and A. M. Nathan, *Phys. Rev. C* **17**, 280 (1978).
- ⁵⁰K. W. Jones, W. R. Harris, M. T. McEllistrem, and D. E. Alburger, *Phys. Rev.* **186**, 978 (1969).
- ⁵¹D. E. Alburger and D. R. Goosman, *Phys. Rev. C* **10**, 935 (1974).
- ⁵²J. E. Esterl, J. C. Hardy, R. G. Sextro, and J. Cerny, *Phys. Lett.* **33B**, 287 (1970).
- ⁵³I. S. Towner, *Nucl. Phys.* **A216**, 589 (1973).
- ⁵⁴J. C. Adloff, K. H. Souw, and C. L. Cocke, *Phys. Rev. C* **3**, 1808 (1971).
- ⁵⁵D. Schwalm and B. Povh, *Nucl. Phys.* **89**, 401 (1966).
- ⁵⁶D. E. Alburger and D. H. Wilkinson, *Phys. Rev.* **153**, 1061 (1967).
- ⁵⁷B. M. K. Nefkens, *Phys. Rev. Lett.* **10**, 243 (1963).
- ⁵⁸A. H. Wapstra, A. Audi, and K. Bos, December 1983 Atomic Mass Adjustments, Nuclear Data Group, Brookhaven National Laboratory; *Nucl. Phys.* **A432**, 1 (1985).
- ⁵⁹D. Bodansky, S. F. Eccles, and I. Halpern, *Phys. Rev.* **108**, 1019 (1957).
- ⁶⁰P. R. Christensen and C. L. Cocke, *Nucl. Phys.* **89**, 656 (1966).